J. Fluid Mech. (2015), *vol.* 779, *pp.* 598–621. © Cambridge University Press 2015
doi:10.1017/jfm.2015.436

Mass transfer effects on linear wave propagation in diluted bubbly liquids

D. Fuster[1,†] **and F. Montel**[2]

[1]Sorbonne Universités, UPMC Université Paris 06, CNRS UMR 7190, Institut Jean le Rond d'Alembert, 75005 Paris, France

[2]Total SA, CSTJF, Avenue Larribau, 64018 Pau, France

(Received 25 March 2015; revised 27 June 2015; accepted 26 July 2015; first published online 19 August 2015)

In this article we investigate the importance of mass transfer effects in the effective acoustic properties of diluted bubbly liquids. The classical theory for wave propagation in bubbly liquids for pure gas bubbles is extended to capture the influence of mass transfer on the effective phase speed and attenuation of the system. The vaporization flux is shown to be important for systems close to saturation conditions and at low frequencies. We derive a general expression for the transfer function that relates bubble radius and pressure changes, solving the linear version of the conservation equations inside, outside and at the bubble interface. Simplified expressions for various limiting situations are derived in order to get further insight about the validity of the common assumptions typically applied in bubble dynamic models. The relevance of the vapour content, the mass transfer flux across the interface and the effect of variations of the bubble interface temperature is discussed in terms of characteristic non-dimensional numbers. Finally we derive the various conditions that must be satisfied in order to reach the low-frequency limit solutions where the phase speed no longer depends on the forcing frequency.

Key words: bubble dynamics, condensation/evaporation, phase change

1. Introduction

The effect of bubbles on the process of wave propagation in liquids is an open scientific problem with many application fields such as ultrasonic fluid flow monitoring and geophysics (Kuster & Toksöz 1974; Lynnworth 2013). One family of models typically used for wave propagation in bubbly flows applies for dilute systems. Most of these models (Van Wijngaarden 1968; Chapman & Plesset 1971; Prosperetti 1977; Sangani 1991; Zhang & Prosperetti 1997; Ando, Colonius & Brennen 2009) succeed in reproducing experimental results for frequencies below resonance in situations where the amount of vapour is negligible (Silberman 1957; Cheyne, Stebbings & Roy 1995; Wilson, Roy & Carey 2005; Leroy *et al.* 2008). These theories have recently been improved at frequencies above the bubble natural frequency. For instance, high-frequency corrections have been proposed by Ando *et al.* (2009), while Fuster, Conoir & Colonius (2014) propose correction

† Email address for correspondence: fuster@dalembert.upmc.fr

terms in order to capture direct bubble–bubble interactions based on the results obtained from a full nonlinear model (Fuster & Colonius 2011).

Theoretical models for linear wave propagation in bubbly liquids require one to model the response of a single bubble to an external pressure excitation. This response is obtained through the linearization of the Rayleigh–Plesset equation and the solution of the mass, momentum and energy conservation equations inside the bubble. Expressing the amplitude of the bubble radius oscillation as a function of the external pressure amplitude allows us to define a bubble resonance frequency and damping factor; see Ainslie & Leighton (2011) for a review. These parameters depend on the so-called transfer function, which relates bubble pressure and volume changes in the linear regime. Prosperetti, Crum & Commander (1988) propose an expression capturing the heat transfer exchange between the bubble and its environment, assuming that the bubble interface temperature is constant and neglecting mass transfer effects across the interface. This function can be used to define an effective state equation for the bubble interior of the type $p_b V_b^{\gamma_{eff}} = C$, where p_b is the bubble pressure, V_b is the bubble volume and γ_{eff} is a frequency-dependent effective coefficient that tends to recover the isothermal limit for low frequencies ($\gamma_{eff} = 1$) and the adiabatic response for very large frequencies ($\gamma_{eff} = \gamma$), where γ is the gas polytropic coefficient.

Wave propagation in systems where mass transfer effects become relevant have been mainly investigated for large void fractions far from the diluted limit (Mecredy & Hamilton 1972; Kieffer 1977; Ardron & Duffey 1978; Landau & Lifshitz 1987). For low enough frequencies, Kieffer (1977) and Landau & Lifshitz (1987) derive limiting expressions assuming that the far-field pressure and temperature are related through the saturation conditions. Models accounting for transient heat, mass and momentum transport have been proposed by Mecredy & Hamilton (1972), Ardron & Duffey (1978) and more recently Saurel, Petitpas & Abgrall (2008).

In diluted systems, mass transfer is expected to influence the local bubble response without significantly influencing the far-field temperature, as the liquid plays the role of an infinite energy reservoir for the bubble oscillation. In this case, one needs to derive corrected expressions to relate bubble radius and external pressure changes. Hao & Prosperetti (1999) consider the problem of mass transfer in pure vapour bubbles by assuming saturation inside the bubble at every instant. Preston, Colonius & Brennen (2007) solve the linearized problem of the dynamics of air/vapour bubbles for situations where transient vaporization effects and heat transport in the liquid boundary layer are not controlling mechanisms. Prosperetti & Hao (2002) also discuss interesting phenomena induced by mass transfer on the dynamics of bubbles, and Prosperetti (2015) presents a simplified model for the influence of mass transfer on the sound speed of a gas/vapour bubbly liquid that reveals that mass transfer effects play an important role in the propagation of waves at low frequencies.

The process of wave propagation near saturation conditions for diluted systems has been less investigated experimentally. Coste, Laroche & Fauve (1990) report evidence of a strong decrease of the sound velocity at low void fractions when approaching the saturation curve in diethyl ether. Unfortunately, their study mainly reports data for large void fractions, where the diluted limit conditions are not met.

In this work we extend the classical linear theory for disperse bubbly liquids to include mass transfer effects across the interface and the diffusion of heat in the liquid. The goals of this study are twofold. First, we want to evaluate the influence of the mass transfer process in the bubble dynamic response and to discuss typical assumptions used in the literature. Second, we want to quantify the importance of

mass transfer effects on the effective acoustic properties of the medium. To that end, the full model that accounts for transient mass transfer effects is presented in § 2. In § 3 we present the linearization procedure followed to derive the expressions for the bubble resonance frequency, damping factor, mass transfer flux, interface temperature variations and effective sound phase speed and attenuation of the gas/vapour–liquid mixture (in the following we will simply name them phase speed and attenuation). In § 4 we present a summary of the model. Section 5 presents some numerical results to gain further insight about mass transfer effects in the process of wave propagation, discussing the relevance of various mechanisms on the bubble response as a function of the vapour content and frequency. Section 6 derives low-frequency limiting solutions, and the conclusions are presented in § 7.

2. Full model

The linearized equations for wave propagation in bubbly media can be derived from basic principles using the conservation equations applied to the averaged mixture. Typically, the 'separation of scales' assumption is used to write the averaged equations for the large-scale wave propagation problem. Thus, neglecting the influence of liquid viscosity at large scales, we write the mass and momentum conservation equations as

$$\frac{1}{\rho c^2}\frac{\mathrm{D}p}{\mathrm{D}t} + \nabla \cdot \boldsymbol{v} = \frac{\partial \beta}{\partial t}, \tag{2.1}$$

$$\rho \frac{\mathrm{D}\boldsymbol{v}}{\mathrm{D}t} = -\nabla p, \tag{2.2}$$

where t is the time coordinate, $\boldsymbol{v}$ is the fluid velocity, p is the pressure and ρ is the average density defined in terms of the void fraction β, the liquid's density ρ_l and the bubble's density ρ_b as $\rho = (1-\beta)\rho_l + \beta\rho_b$. The void fraction β is defined using a probabilistic function for the bubble equilibrium radius, $f(a)$, and the number of bubbles per unit volume, n,

$$\beta = \frac{4}{3}\pi n \int_0^\infty a^3 f(a)\,\mathrm{d}a. \tag{2.3}$$

The system of equations above requires to derive an equation to relate external pressure changes with the local bubble radius variation. This equation is found by solving the conservation equations inside and outside the bubble at the local scale. If we impose spherical symmetry for the bubble oscillation, the basic equations for a system of N species can be written as

$$\frac{\mathrm{D}\rho}{\mathrm{D}t} + \frac{\rho}{r^2}\frac{\partial (v_r r^2)}{\partial r} = 0, \tag{2.4}$$

$$\rho \frac{\mathrm{D}Y_i}{\mathrm{D}t} = -\frac{1}{r^2}\frac{\partial}{\partial r}(r^2 J_i^{diff}), \tag{2.5}$$

$$\rho \frac{\mathrm{D}v_r}{\mathrm{D}t} = -\frac{\partial p}{\partial r} + \frac{1}{r^2}\frac{\partial r^2 \tau_{rr}}{\partial r} - \frac{\tau_{\theta\theta} + \tau_{\phi\phi}}{r}, \tag{2.6}$$

$$\rho \frac{\mathrm{D}e}{\mathrm{D}t} = -\frac{p}{r^2}\frac{\partial (v_r r^2)}{\partial r} - \frac{1}{r^2}\frac{\partial (r^2 q_r)}{\partial r} + \phi_v, \tag{2.7}$$

where r is the radial coordinate, Y_i is the mass fraction of the ith component, j_i^{diff} is the diffusive mass flux, p is the pressure, T is temperature, $\boldsymbol{\tau}$ is the viscous stress tensor, e is the specific internal energy, q_r is the radial heat flux and ϕ_v is the viscous dissipation function. These equations apply for both the gas/vapour mixture inside the bubble and the liquid surrounding it.

The ideal gas equation is a good approximation of the real equation of state for both gas and vapour components inside the bubble in standard conditions. In the liquid, the definition of the sound speed in a pure liquid is typically used to relate pressure and density variations. Using the Fourier and Fick laws to express the diffusive heat and mass flux, and neglecting the enthalpy difference between the different components of the mixture at a given temperature, we obtain the following set of equations that apply both inside and outside the bubble:

$$\frac{\mathrm{D}\rho_m}{\mathrm{D}t} + \frac{\rho_m}{r^2}\frac{\partial (v_m r^2)}{\partial r} = 0, \tag{2.8}$$

$$\rho_m \frac{\mathrm{D}Y_{i,m}}{\mathrm{D}t} = \frac{1}{r^2}\frac{\partial}{\partial r}\left(r^2 D^M_{i/m}\frac{\partial Y_{i,m}}{\partial r}\right), \tag{2.9}$$

$$\rho_m \frac{Dv_m}{Dt} = -\frac{\partial p_m}{\partial r}, \tag{2.10}$$

$$\rho_m c_{p,m}\frac{\mathrm{D}T_m}{\mathrm{D}t} = \alpha_V T_m \frac{\mathrm{D}p_m}{\mathrm{D}t} + \frac{1}{r^2}\frac{\partial}{\partial r}\left(r^2\kappa_m\frac{\partial T_m}{\partial r}\right) + \frac{4}{3}\mu_m\left(\frac{\partial v_m}{\partial r} - \frac{v_m}{r}\right)^2. \tag{2.11}$$

Here $c_{p,m}$ is the average specific heat, α_V is the thermal dilatation coefficient, which is $\alpha_V = 1/T_m$ for an ideal gas and approximately zero for liquids, κ_m is the average conductivity and $D^M_{i/m}$ is the diffusion coefficient of the ith component in the mixture. The subindex m is used to denote the average mixture properties. When the equations are applied inside the bubble, the subindex m will be replaced by b; when applied to the liquid, we will use the subindex l.

The boundary conditions used to solve the system above can be found, for example, in Hauke, Fuster & Dopazo (2007). At the bubble centre, spherical symmetry imposes the radial gradients to be zero (i.e. $\partial Y_{i,b}/\partial r = \partial \rho_b/\partial r = \partial T_b/\partial r = 0$). The bubble velocity is also set to zero, $v_b(r=0, t) = 0$.

Far from the bubble, pressure, temperature and all the species concentrations in the liquid are assumed to be known ($p_{l,\infty}$, T_0, $Y_{i,l,0}$).

The local balances at the infinitely thin interface relate the liquid and gas properties at both sides of the interface. The mass balance across the bubble is

$$J = \rho_g(\dot{R} - v_b^I) = \rho_l(\dot{R} - v_l^I) \quad \text{at } r = R, \tag{2.12}$$

where J is the total evaporation mass flux across the interface, R is the bubble radius, $\dot{R}$ is the interface velocity, and v_b^I and v_l^I denote respectively the fluid interface velocity in the bubble and in the liquid. The momentum balance accounting for mass transfer effects reads

$$J(v_b^I - v_l^I) = p_l^I - p_b^I + \tau_{rr,l} - \tau_{rr,b} + \frac{2\sigma}{R} \quad \text{at } r = R, \tag{2.13}$$

where σ is the surface tension coefficient.

The total flux of the ith component across the interface is calculated as the sum of the advective flux and the diffusive flux. As both fluxes must be equal at $r = R$, we obtain an equation for the conservation of the ith component across the interface as

$$-JY_{i,l} - \rho_l D^M_{i/l} \frac{\partial Y_{i,l}}{\partial r} = -JY_{i,b} - \rho_g D^M_{i/b} \frac{\partial Y_{i,b}}{\partial r} \quad \text{at } r = R. \tag{2.14}$$

The energy balance at the interface establishes the relation among the energy fluxes at the liquid–gas boundaries. This equation can be approximated by using the total latent heat of vaporization, ΔH_{vap}, as

$$\kappa_l \frac{\partial T_l}{\partial r} = \kappa_g \frac{\partial T_g}{\partial r} + \sum_{i=1}^{N} J_i \Delta H_{vap,i} \quad \text{at } r = R, \tag{2.15}$$

where J_i is the flux across the interface of the ith component and $\Delta H_{vap,i}$ is the enthalpy of vaporization related to the phase change. Finally, we assume a continuous temperature profile across the interface so that the interface temperature is equal for both phases ($T_g(r = R) = T_l(r = R) = T_{int}$).

To evaluate the flux of every component across the interface J_i that finally determines the total flux $J = \sum_{i=1}^{N} J_i$, we can either impose equilibrium conditions at the interface at every instant, or assume that the flux is proportional to the difference between the equilibrium state and the current state. In fact, using the kinetic theory of gases, it is possible to obtain the total flux of vapour across the interface using the Hertz–Knudsen–Langmuir expression (Knudsen 1915; Hertz 1982),

$$J_{vap} = \alpha_{evap} \frac{(p^I_{eq} - p^I_{b,vap})}{\sqrt{2\pi r_{vap} T_{int}}}, \tag{2.16}$$

where α_{evap} is the accommodation coefficient, which is a measure of the ratio of the molecules hitting the interface that change the phase, $p^I_{b,vap}$ is the partial pressure of vapour at the interface, r_{vap} is the vapour's perfect gas constant and p^I_{eq} is the equilibrium pressure at the interface conditions. For the vapour, the equilibrium pressure can be obtained from the Clausius–Clapeyron relation,

$$\frac{\mathrm{d}p_{eq}}{\mathrm{d}T} = \Delta H_{vap} \frac{p_{eq}}{r_{vap} T^2}. \tag{2.17}$$

It is interesting to remark that the system of equations above simplifies in cases where the interface is assumed to be at equilibrium at every instant. As we will prove along the theoretical development, for low enough frequencies, transient mass transfer effects (2.16) are not relevant. In this situation the total flux is given by diffusion, assuming equilibrium conditions at the interface at every instant. Analogously, the model could be easily extended for soluble gases by using the equilibrium pressure (or concentration) given by Henry's law. It must be noted that in this work we will not consider the presence of soluble gases in the liquid given that the mass and heat flux related to phase change of soluble components is usually negligible compared with that of vapour.

3. Linearized solutions

The set of equations described above can be simplified assuming that all variables oscillate around an equilibrium state with a given frequency ω. Thus, for a given variable y, we look for solutions of the form $y = y_0(1 + \Delta y \mathrm{e}^{\mathrm{i}\omega t})$, where Δy is a complex quantity to be determined. For the linear solution to be valid, $\Delta y \ll 1$.

At the local scale, the momentum and continuity equations in the liquid can be rewritten as the Rayleigh–Plesset equation, which relates pressure (or potential) variations induced by the far field with the local response of the bubble. Neglecting compressibility effects, the modified Rayleigh–Plesset equation accounting for mass transfer effects reads (Prosperetti 1982)

$$R\ddot{R} - \frac{R\dot{J}}{\rho_l} + \frac{3}{2}\left(\dot{R} - \frac{J}{\rho_l}\right)^2 - 2\frac{J}{\rho_l}\left(\dot{R} - \frac{J}{\rho_l}\right) = \frac{p_l^I - p_{l,\infty}}{\rho_l}, \tag{3.1}$$

where p_l^I can be expressed in terms of the properties inside the bubble using (2.13). In the following, we will consider the system of a bubble containing an immiscible gas and a vapour with an equilibrium concentration Y_0 in a one-component liquid. This is representative of most of the gas–liquid systems, as the most important flux across the interface is expected to be given by liquid vaporization. In the linear limit the flux across the interface is $J = J_0 \Delta R \mathrm{e}^{\mathrm{i}\omega t}$, where J_0 is a complex quantity to be determined. Neglecting nonlinear terms we simplify the modified Rayleigh–Plesset equation as

$$-R_0^2\omega^2\Delta R - \frac{R_0 J_0 \mathrm{i}\omega}{\rho_l}\Delta R = \frac{\Delta R}{\rho_l}\left(-p_{b,0}\Phi + \frac{2\sigma}{R_0} - 4\mu_l \mathrm{i}\omega\right) - \frac{p_{l,0}\Delta p_\infty}{\rho_l}, \tag{3.2}$$

where Φ is a complex function to be obtained that is typically named the transfer function and it serves to relate bubble radius oscillations and internal bubble pressure variations, such that $\Delta p_b = -\Phi \Delta R$.

The equation above can be rearranged to express the bubble radius variations in terms of the far-field pressure variations as

$$\Delta R = -\frac{1}{\omega_0^2 - \omega^2 + 2\mathrm{i}\delta\omega}\Delta p_\infty \frac{p_{l,0}}{\rho_l R_0^2}, \tag{3.3}$$

where

$$\delta = \frac{2\mu_l}{\rho_l R_0^2} + \frac{p_{g,0}}{2\omega\rho_l R_0^2}\,\mathrm{Im}(\Phi) + \frac{\mathrm{Re}(J_0)}{2\rho_l R_0}, \tag{3.4}$$

$$\omega_0^2 = \frac{p_{g0}}{\rho_l R_0^2}\left(\mathrm{Re}(\Phi) - \frac{2\sigma}{p_{g,0}R_0}\right) + \frac{\omega\,\mathrm{Im}(J_0)}{\rho_l R_0}. \tag{3.5}$$

Equations (3.4) and (3.5) require the evaluation of the transfer function Φ and the flux across the interface J_0. Both variables can be obtained from the solution of the conservation equations inside the bubble. Following a development similar to that of Commander & Prosperetti (1989), we consider a perfect gas and uniform pressure inside the bubble. The continuity equation inside the bubble can be rewritten using the energy equation as

$$\frac{\dot{p}_b}{\gamma p_b} + \nabla \cdot \left(v_b - \frac{\gamma - 1}{\gamma p_b}\kappa_b \nabla T_b\right) = 0. \tag{3.6}$$

Integrating the equation from the bubble centre to a given distance r, the radial velocity inside the bubble is given by

$$v_b(r) = \frac{1}{\gamma p}\left((\gamma-1)\kappa_b\frac{\partial T}{\partial r} - \frac{1}{3}\dot{p}_b r\right). \tag{3.7}$$

This equation is evaluated at the interface to find an expression for the bubble's internal pressure,

$$\dot{p}_b = \frac{3}{R}(\gamma-1)\kappa_b \left.\frac{\partial T_b}{\partial r}\right|_{r=R} - \frac{3}{R}\gamma p_b v_b^I. \tag{3.8}$$

Using (2.12) to express the gas/vapour velocity at the interface (v_b^I) as a function of the total evaporation flux and the interface velocity and linearizing, we obtain

$$\Delta p_b = -3(\gamma-1)\mathrm{i}Pe_b^{-1}\frac{\gamma}{\gamma-1}\left.\frac{\partial \Delta T_b}{\partial \zeta}\right|_{\zeta=1} - 3\gamma\Delta R - 3\gamma\mathrm{i}J_0^*\Delta R, \tag{3.9}$$

where $\zeta = r/R$ is the non-dimensional radial distance, $Pe_b = \omega R_0^2/D_b^T$ is the bubble's Péclet number defined using the bubble's thermal diffusivity D_b^T, and the non-dimensional mass transfer flux is

$$J_0^* = \frac{J_0}{\rho_{b,0}R_0\omega}. \tag{3.10}$$

Assuming that only one component (denoted with the subindex w) is vaporized and that the vapour pressure depends solely on temperature, we can evaluate the mass transfer flux from the linearization of (2.16) to obtain

$$J_0^*\Delta R = J_{max}^*\left[\frac{\partial p_{eq}}{\partial T}\frac{T_0}{p_{eq}}\Delta T_b(\zeta=1) - \Delta p_b + \Delta Y(\zeta=1)\right], \tag{3.11}$$

where J_{max}^* is a non-dimensional flux defined as

$$J_{max}^* \equiv \alpha_{evap}\frac{p_{eq,0}}{\rho_{b,0}R_0\omega\sqrt{2\pi r_w T_0}}. \tag{3.12}$$

Equation (3.11) requires knowledge of the vapour mass fraction variations and the temperature variations at the interface. To obtain $\Delta Y(\zeta=1)$ we solve the linear transport equation for the vapour inside the bubble. The transport equation (2.9) is written in a non-dimensional form using the Sherwood number, $Sh_D = \omega R_0^2/D_{w/b}$, where $D_{w/b}$ is the diffusion coefficient of the vapour inside the bubble mixture,

$$Sh_D\Delta Y + \mathrm{i}\frac{1}{\zeta^2}\frac{\partial}{\partial\zeta}\left(\zeta^2\frac{\partial\Delta Y}{\partial\zeta}\right) = 0. \tag{3.13}$$

Its general solution,

$$\Delta Y(\zeta) = C_D\frac{\sinh(\sqrt{Sh_D\mathrm{i}}\zeta)}{\zeta}, \tag{3.14}$$

is particularized using the boundary condition for component w at the interface (2.14),

$$-J_0^*\Delta R = -J_0^*Y_0\Delta R - Sh_D^{-1}Y_0\left.\frac{\partial\Delta Y}{\partial\zeta}\right|_{\zeta=1}, \tag{3.15}$$

where we have imposed $Y_{w,l} = 1$. Thus, we can determine the constant C_D to write the evolution of the mass fraction at the interface as

$$\Delta Y(\zeta = 1) = J_0^* \frac{Sh_D}{\sqrt{\mathrm{i}Sh_D}\coth(\sqrt{\mathrm{i}Sh_D}) - 1} \frac{1 - Y_0}{Y_0} \Delta R. \tag{3.16}$$

The temperature variations at the interface are obtained using the energy equation inside the bubble ((2.11)). The non-dimensional linear version of this equation,

$$\Delta T_b - \Delta p_b \frac{\gamma - 1}{\gamma} + \mathrm{i}Pe_b^{-1} \frac{1}{\zeta^2} \frac{\partial}{\partial \zeta} \left(\zeta^2 \frac{\partial \Delta T_b}{\partial \zeta} \right) = 0, \tag{3.17}$$

has the following general solution:

$$\Delta T_b(\zeta) = \Delta p_b \frac{\gamma - 1}{\gamma} + C_1 \frac{\exp(-\sqrt{Pe_b \mathrm{i}}\zeta)}{\zeta} + C_2 \frac{\exp(\sqrt{Pe_b \mathrm{i}}\zeta)}{\zeta}. \tag{3.18}$$

Because the temperature is finite at $\zeta = 0$, we find that $C_1 = -C_2 = -C_0/2$. Thus, the interface's temperature variation is given by

$$\Delta T_b(\zeta = 1) = \Delta p_b \frac{\gamma - 1}{\gamma} + C_0 \sinh(\sqrt{Pe_b \mathrm{i}}). \tag{3.19}$$

Plugging (3.16) and (3.19) into (3.11) we obtain the following explicit relation for the mass flux across the interface:

$$J_0^* \Delta R = J_c^* \left((\Delta H_{vap}^* - 1) \Delta p_b + \Delta H_{vap}^* \frac{\gamma}{\gamma - 1} C_0 \sinh(\sqrt{Pe_b \mathrm{i}}) \right), \tag{3.20}$$

where we have defined a non-dimensional enthalpy of vaporization as $\Delta H_{vap}^* = (\Delta H_{vap}/c_{p,b}T_0)$ and a characteristic non-dimensional flux,

$$J_c^* = \frac{J_{max}^*}{1 + J_{max}^* \dfrac{Sh_D}{\sqrt{\mathrm{i}Sh_D}\coth(\sqrt{\mathrm{i}Sh_D}) - 1} \dfrac{1 - Y_0}{Y_0}}. \tag{3.21}$$

Note that this quantity provides a quantification of the influence of transient mass transfer effects. In fact, we can write (3.21) using the characteristic non-dimensional mass flux $J_{c,eq}^*$ that is obtained by assuming that equilibrium conditions prevail at the interface at every instant (see appendix A for details of the derivation of $J_{c,eq}^*$),

$$J_c^* = \frac{J_{max}^*}{1 + J_{max}^* (J_{c,eq}^*)^{-1}}. \tag{3.22}$$

When the characteristic mass flux related to transient effects is much faster than that at equilibrium conditions ($J_{max}^* \gg J_{c,eq}^*$), the mass transfer is controlled by vapour diffusion inside the bubble: $J_c^* \approx J_{c,eq}^*$. In the opposite limit ($J_{max}^* \ll J_{c,eq}^*$), transient mass transfer effects control the mass flux across the interface: $J_c^* \approx J_{max}^*$.

To obtain the value of the integration constant C_0 in (3.20), one needs to solve the energy equation (2.11) in the liquid. In its linearized form this equation reads

$$\Delta T_l = -\mathrm{i}Pe_l^{-1} \frac{1}{\zeta^2} \frac{\partial}{\partial \zeta} \left(\zeta^2 \frac{\partial \Delta T_l}{\partial \zeta} \right), \tag{3.23}$$

and its general solution is

$$\Delta T_l(\zeta) = C_3 \frac{\exp\left(-\sqrt{Pe_l \mathrm{i}}\zeta\right)}{\zeta} + C_4 \frac{\exp\left(\sqrt{Pe_l \mathrm{i}}\zeta\right)}{\zeta}, \tag{3.24}$$

where $Pe_l = \omega R_0^2 / D_l^T$ is the liquid's Péclet number. Note that, consistent with the derivation of the far-field equations, the effect of viscous dissipation as well as thermal dilatation on the temperature variations have been neglected. The particular solution of this equation requires one to evaluate the liquid's temperature at some distance ζ_∞. In the dilute limit, one can consider that the temperature far from the bubble is constant and equal to T_0. In this case we find $C_4 = 0$.

The values of the free constants C_3 and C_0 in (3.19) and (3.24) are obtained by applying the boundary conditions at the interface. First, we assume that the interface's temperature has to be continuous. Thus we write

$$C_3 \exp(-\sqrt{Pe_l \mathrm{i}}) = \Delta p_b \frac{\gamma - 1}{\gamma} + C_0 \sinh\left(\sqrt{Pe_b \mathrm{i}}\right). \tag{3.25}$$

In addition, the energy balance across the interface (2.15) establishes that

$$\left.\frac{\partial \Delta T_l}{\partial \zeta}\right|_{\zeta=1} = \frac{\kappa_b}{\kappa_l} \left.\frac{\partial \Delta T_b}{\partial \zeta}\right|_{\zeta=1} + J_0^* Pe_b \Delta H_{vap}^* \Delta R. \tag{3.26}$$

Replacing the corresponding expressions for the temperature derivatives and using (3.25) to express C_3 as a function of C_0, we obtain

$$C_0 = -\frac{\dfrac{\gamma - 1}{\gamma}(1 - \Delta T_c^I)}{\sinh\left(\sqrt{Pe_b \mathrm{i}}\right)} \Delta p_b, \tag{3.27}$$

where the complex quantity ΔT_c^I is defined as

$$\Delta T_c^I = \frac{\kappa_b}{\kappa_l} \frac{\sqrt{Pe_b \mathrm{i}} \coth\left(\sqrt{Pe_b \mathrm{i}}\right) - 1 + J_c^* Pe_b \Delta H_{vap}^* \left(\dfrac{\gamma}{\gamma - 1}\right)}{1 + \sqrt{Pe_l \mathrm{i}} + \dfrac{\kappa_b}{\kappa_l}\left[\sqrt{Pe_b \mathrm{i}} \coth\left(\sqrt{Pe_b \mathrm{i}}\right) - 1 + J_c^* Pe_b (\Delta H_{vap}^*)^2 \dfrac{\gamma}{\gamma - 1}\right]}. \tag{3.28}$$

Upon substitution of the integration constant into (3.25), we can represent the temperature variations at the interface as

$$\Delta T_b(\zeta = 1) = \frac{\gamma - 1}{\gamma} \Delta T_c^I \Delta p_b. \tag{3.29}$$

The temperature gradient inside the bubble evaluated at the interface is obtained from (3.19),

$$\left.\frac{\partial \Delta T_b}{\partial \zeta}\right|_{\zeta=1} = -\frac{\gamma - 1}{\gamma}(1 - \Delta T_c^I)[\sqrt{Pe_b \mathrm{i}} \coth\left(\sqrt{Pe_b \mathrm{i}}\right) - 1] \Delta p_b, \tag{3.30}$$

and the mass flux across the interface (3.20) is expressed as a function of the bubble pressure variations as

$$J_0^* \Delta R = J_c^* (\Delta H_{vap}^* \Delta T_c^I - 1) \Delta p_b. \tag{3.31}$$

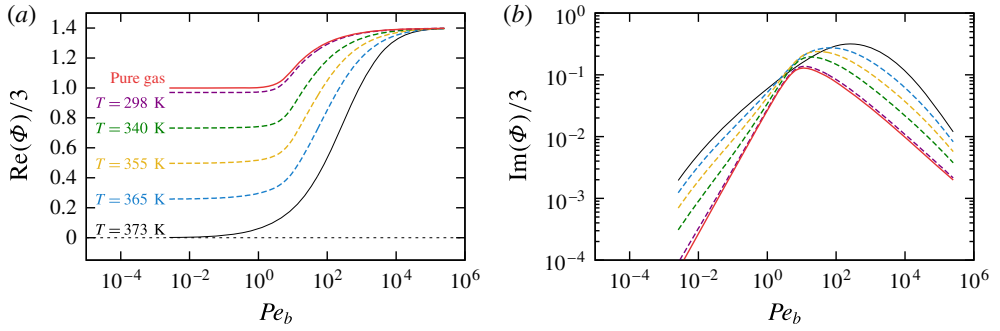

FIGURE 1. (Colour online) Influence of the vapour content on the real (*a*) and imaginary (*b*) parts of the transfer function (3.32) for various Péclet numbers. The values of the non-dimensional quantities J_c^*, ΔH_{vap}^* and ΔT_c^I are obtained for a 100 μm air/water vapour bubble at 1 atm and varying temperature (from 25 to 100 °C). The vapour content for the various curves are $Y_0 = 0$, 0.03, 0.27, 0.50, 0.74 and 0.99.

Replacing the expressions for the temperature gradient and mass flux ((3.30) and (3.31)) into (3.9), we finally obtain the transfer function Φ as

$$\Phi = \frac{3\gamma}{1 - 3(\gamma - 1)\mathrm{i}Pe_b^{-1}[\sqrt{Pe_b\mathrm{i}}\coth(\sqrt{Pe_b\mathrm{i}}) - 1](1 - \Delta T_c^I) + 3\gamma\mathrm{i}J_c^*(\Delta H_{vap}^*\Delta T_c^I - 1)}. \tag{3.32}$$

This transfer function is a generalization of the classical expression for pure gas bubbles (Prosperetti *et al.* 1988) accounting for interface temperature variations and mass transfer effects across the interface. For instance, it is easy to check that we recover the classical solution for pure gas bubbles by imposing no net mass flux across the interface ($J_c^* = 0$) and by assuming that the interface temperature variations are zero ($\Delta T_c^I = 0$).

Figure 1 depicts the real and imaginary parts of the transfer function obtained for an air/vapour bubble for various water vapour contents at constant atmospheric pressure. At high frequencies, the bubbles tend to recover the adiabatic response irrespective of the vapour content. At low frequencies, the transfer function recovers the isothermal limit for pure gas bubbles. As the amount of vapour increases, the real part takes values below 1 at low frequencies. This value corresponds to the limiting case in which equilibrium conditions prevail inside the bubble at every instant. It can be proven that this result can also be found by assuming that vapour and gas are both ideal gases at constant temperature (see appendix B). The imaginary part is also influenced by the vapour content. In general the imaginary part increases with the vapour content irrespective of the Péclet number, although the influence of the vapour content on the imaginary part is especially notorious at low frequencies. Consistent with experimental observations, the influence of vaporization is completely negligible in gas/vapour bubbles under standard laboratory conditions (25 °C and 1 atm), where the vapour void fraction is negligible compared with that of a gas.

Once we have obtained expressions for the transfer function (3.32) and the mass flux across the interface (3.31), we follow the classical procedure to linearize the averaged continuity and momentum equations ((2.1) and (2.2)) written as a wave

equation of the form

$$\frac{1}{c_{eff}^2}\frac{\partial^2 p_{l,\infty}}{\partial t^2} - \Delta p_{l,\infty} = 4\pi\rho \int_0^\infty a^2 \ddot{R} f(a)\,\mathrm{d}a, \tag{3.33}$$

where $\ddot{R} = -\omega^2 R_0 \Delta R$ is the interface acceleration. Rewriting (3.33) as a wave equation for $p_{l,\infty}$, the complex sound speed, c_m, is given by

$$\frac{1}{c_m^2} = \frac{1}{c^2} + 4\pi n \int_0^\infty \frac{a f(a)\,\mathrm{d}a}{\omega_0^2 - \omega^2 + 2\mathrm{i}\delta\omega}, \tag{3.34}$$

from which we obtain the phase velocity, c_{ph}, and attenuation, Q^{-1}, as

$$c_{ph} = \left(\mathrm{Re}\left(\frac{1}{c_m}\right)\right)^{-1}, \tag{3.35}$$

$$Q^{-1} = -20\log_{10}(e)\,\mathrm{Im}\left(\frac{\omega}{c_m}\right). \tag{3.36}$$

Using the expressions for the bubble resonant frequency and damping constant (3.4) and (3.5), we obtain the phase speed (3.35) and attenuation (3.36).

4. Summary of equations

As a summary of the full model equations for a bubbly liquid with vapour and an inmiscible gas, we solve for the averaged complex sound speed,

$$\frac{1}{c_m^2} = \frac{1}{c^2} + 4\pi n \int_0^\infty \frac{a f(a)\,\mathrm{d}a}{\omega_0^2 - \omega^2 + 2\mathrm{i}\delta\omega}, \tag{4.1}$$

in order to obtain the phase speed and attenuation as

$$c_{ph} = \left(\mathrm{Re}\left(\frac{1}{c_m}\right)\right)^{-1}, \tag{4.2}$$

$$Q^{-1} = -20\log_{10}(e)\,\mathrm{Im}\left(\frac{\omega}{c_m}\right). \tag{4.3}$$

The second term in (4.1) represents the influence of the bubble oscillation on the large-scale wave propagation problem, and it can be obtained in the linear regime by solving the conservation equations at the local scale (single bubble and its surrounding liquid). From the linearization of the Rayleigh–Plesset equation (e.g. continuity and momentum equation in the surrounding liquid), we find the following expressions for the bubble resonant frequency and the damping coefficient:

$$\delta = \frac{2\mu_l}{\rho_l R_0^2} + \frac{p_{g,0}}{2\omega\rho_l R_0^2}\,\mathrm{Im}(\Phi) + \frac{1}{2}\mathrm{Re}(J_0^*)\frac{\rho_b}{\rho_l}\omega, \tag{4.4}$$

$$\omega_0^2 = \frac{p_{g0}}{\rho_l R_0^2}\left(\mathrm{Re}(\Phi) - \frac{2\sigma}{p_{g,0}R_0}\right) + \mathrm{Im}(J_0^*)\frac{\rho_b}{\rho_l}\omega^2. \tag{4.5}$$

These properties require the evaluation of the non-dimensional mass transfer flux J_0^* and the transfer function Φ that relate the bubble's pressure and volume changes.

From the solution of the conservation equations inside the bubble and the energy equation in the surrounding liquid, we find the following expressions for these two quantities:

$$J_0^* = J_c^*(1 - \Delta H_{vap}^* \Delta T_c^l)\Phi, \tag{4.6}$$

$$\Phi = \frac{3\gamma}{1 - 3(\gamma - 1)\mathrm{i}Pe_b^{-1}[\sqrt{Pe_b\mathrm{i}}\coth(\sqrt{Pe_b\mathrm{i}}) - 1](1 - \Delta T_c^l) + 3\gamma\mathrm{i}J_c^*(\Delta H_{vap}^* \Delta T_c^l - 1)}. \tag{4.7}$$

Here $Pe_b = \omega R_0^2/D_b^T$, $\Delta H_{vap}^* = \Delta H_{vap}/c_{p,b}T_0$, and J_c^* and ΔT_c^l are the characteristic non-dimensional flux and the non-dimensional interface temperature variation. The general expression for the non-dimensional flux J_c^*,

$$J_c^* = \frac{J_{max}^*}{1 + J_{max}^*(J_{c,eq}^*)^{-1}}, \tag{4.8}$$

reveals that the total flux across the interface can be controlled either by vapour diffusion inside the bubble, $J_{c,eq}^*$, or by transient vaporization effects across the interface, J_{max}^*. The diffusion flux,

$$J_{c,eq}^* = \frac{\sqrt{\mathrm{i}Sh_D}\coth(\sqrt{\mathrm{i}Sh_D}) - 1}{Sh_D}\frac{Y_0}{1 - Y_0}, \tag{4.9}$$

depends on the Sherwood number $Sh_D = \omega R_0^2/D_{w/b}$ and the amount of vapour Y_0. The characteristic transient mass flux is

$$J_{max}^* = \alpha_{evap}\frac{p_{eq,0}}{\rho_{b,0}R_0\omega\sqrt{2\pi r_w T_0}}. \tag{4.10}$$

Finally, the non-dimensional interface temperature variation is a complex function depending on the heat and mass transfer processes taking place at the local scale and its general solution is

$$\Delta T_c^l = \frac{\kappa_b}{\kappa_l}\frac{\sqrt{Pe_b\mathrm{i}}\coth(\sqrt{Pe_b\mathrm{i}}) - 1 + J_c^* Pe_b \Delta H_{vap}^*\left(\dfrac{\gamma}{\gamma - 1}\right)}{1 + \sqrt{Pe_l\mathrm{i}} + \dfrac{\kappa_b}{\kappa_l}\left[\sqrt{Pe_b\mathrm{i}}\coth(\sqrt{Pe_b\mathrm{i}}) - 1 + J_c^* Pe_b(\Delta H_{vap}^*)^2\dfrac{\gamma}{\gamma - 1}\right]}, \tag{4.11}$$

where $Pe_l = \omega R_0^2/D_l^T$.

In the following sections, we discuss the importance of mass transfer in the bubble dynamic response and the wave propagation properties of the effective medium as well as simplified solutions for limiting situations.

5. The influence of mass transfer effects on the acoustic properties of the effective medium

In this section we evaluate the importance of mass transfer effects in a system by comparing the results obtained using the full model with those provided by the classical linear theory, which neglects mass transfer effects. We consider a mixture of monodisperse bubbles with average radius 100 μm and bubble concentration of

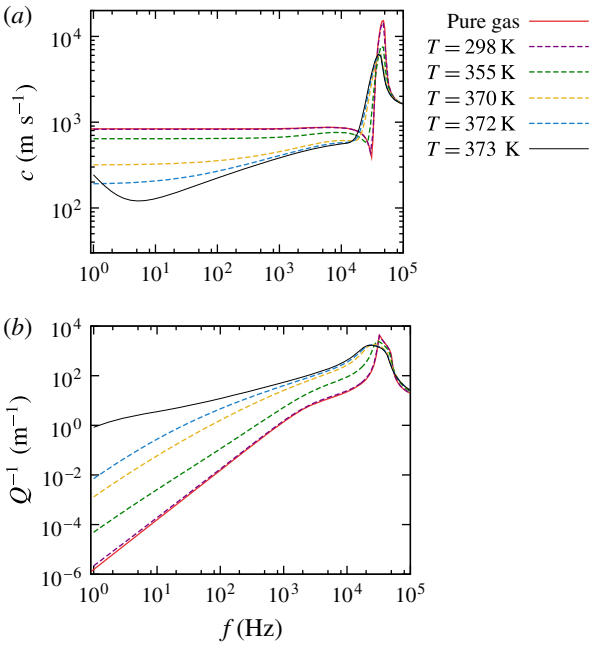

FIGURE 2. (Colour online) Influence of the vapour content on the phase velocity (*a*) and attenuation (*b*) curves obtained from the set of equations summarized in § 4 for gas/vapour bubbles at 1 atm and various ambient temperatures. The vapour content for each condition is $Y_0 = 0.99$, 0.96, 0.89, 0.55 and 0.03. For reference, the red line represents the solution for pure air bubbles ($Y_0 = 0$) at 1 atm and 25 °C. Mass transfer effects significantly modify both phase speed and attenuation curves for frequencies below resonance. In the low-frequency limit, mass transfer decreases the phase velocity and increases attenuation.

$\beta_0 = 10^{-4}$ (vol/vol) measured at standard temperature (25 °C) and pressure (1 atm). We take the physical properties of an air–water system. Because the exact value of the accommodation coefficient is not clear yet (Gumerov, Hsiao & Goumilevski 2001), in this work we have taken $\alpha_{evap} = 0.35$ (Yasui 1997; Hauke *et al.* 2007; Fuster, Hauke & Dopazo 2010), where we have neglected any influence of the temperature on this parameter.

Figure 2 contains the effective phase velocity and attenuation as functions of the vapour content and frequency obtained with the full model. The vapour content is controlled by varying the ambient temperature from 25 °C to the normal boiling point of water (100 °C) at constant ambient pressure. Under these conditions, the classical theory which neglects mass transfer effects does not predict any significant influence of the vapour content (or ambient temperature) on the results obtained. However, the results obtained with the full model reveal that mass transfer effects become relevant at low frequencies for bubbles with a large vapour content. At low frequencies the phase velocity is significantly reduced with respect to the value predicted when neglecting mass transfer effects, whereas attenuation values increase by various orders of magnitude. The analysis of low-frequency asymptotic solutions reached for low frequencies is postponed to the next section.

The differences in the formulation of the full model including mass transfer effects with respect to the classical formulation for pure gas bubbles can be condensed into

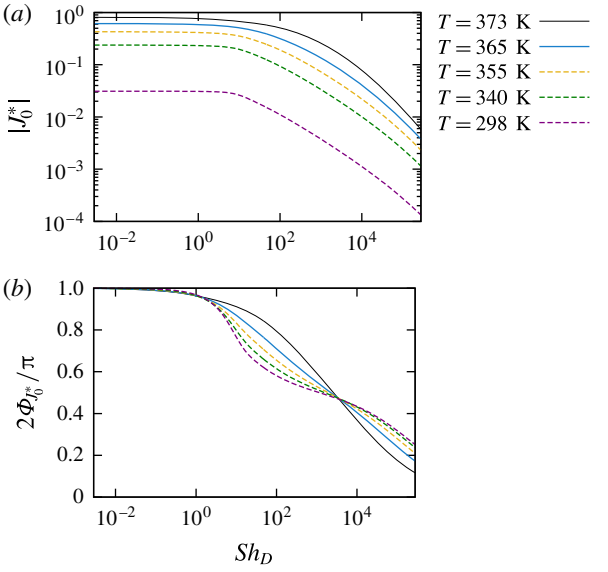

FIGURE 3. (Colour online) (*a*) Non-dimensional evaporation flux (4.6) as a function of the vapour content (varied by changing the ambient temperature at a constant pressure equal to 1 atm) and the Sherwood number. (*b*) Phase lag between the bubble radius and flux oscillation as a function of the vapour content and the Sherwood number.

two non-dimensional quantities: J_0^* as defined in (3.10), which is interpreted as the ratio between the interface velocity induced by mass transfer $(J_0/\rho_b)\Delta R$ and the actual interface velocity $R_0\omega\Delta R$; and ΔT_c^I as defined in (3.28), which is a measure of the non-dimensional temperature variations at the interface (3.29). When J_0^* is close to unity, mass transfer controls the evolution of the bubble radius, whereas when it is smaller than unity, the gas/vapour expansion controls the bubble radius evolution.

Figure 3 shows the modulus and the phase lag with respect to the bubble radius oscillations of the non-dimensional mass transfer flux as a function of the Sherwood number and the vapour content (varied by changing the ambient temperature from 25 to 100 °C at 1 atm). For a given vapour content, the evaporation flux reaches an asymptotic limit for low Sherwood numbers (low frequencies), which corresponds to the limit obtained assuming thermodynamic equilibrium inside the bubble at every instant (appendix B). This low-frequency limit is also the maximum mass transfer flux across the interface for a given vapour content. Only for systems approaching saturation conditions does the non-dimensional mass transfer flux become of order unity, meaning that evaporation and condensation processes take control of the dynamic response of the interface. On the contrary, for $Sh_D \gg 1$, the bubble has almost no time to respond to pressure waves and the evaporation flux becomes negligible. In this high-frequency regime, neither phase speed nor attenuation are significantly influenced by mass transfer effects, and we can conclude that the bubble dynamic response is governed by the gas/vapour expansion or compression.

The relevance of the interface temperature variations is captured by the non-dimensional quantity ΔT_c^I. Figure 4 shows ΔT_c^I as a function of the bubble's Péclet number, the non-dimensional enthalpy of vaporization and the amount of vapour, which ultimately controls the mass flux across the interface. As expected, the interface temperature variations are negligible when the vapour content is low, irrespective of

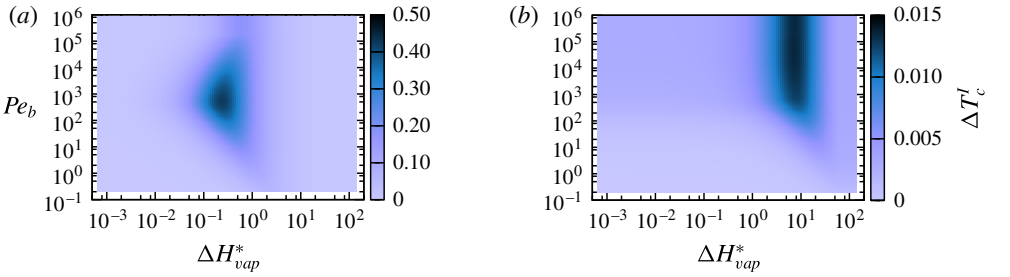

FIGURE 4. (Colour online) Dimensionless interface temperature variations (4.11) as a function of the non-dimensional enthalpy of vaporization, ΔH^*_{vap}, and the bubble Péclet number, Pe_b, for a 100 μm bubble with large vapour content $Y_0 = 0.99$ (*a*) and low vapour content $Y_0 = 0.05$ (*b*).

the forcing frequency and enthalpy of vaporization. In this case, the energy exchange due to evaporation or condensation is not significant. As we approach saturation conditions, the mass flux across the interface and the associated energy exchange make the interface temperature variations important. The sensitivity is maximal for a given enthalpy of vaporization that depends slightly on the forcing frequency. For reference, in the particular case of water, the non-dimensional enthalpy of vaporization, ΔH^*_{vap}, takes values of order unity, meaning that the interface temperature variations become important near saturation conditions. Regarding the frequency, the interface temperature variations are not important at low frequencies for both gas and vapour bubbles, as the bubble has enough time to equilibrate its temperature with the surrounding liquid at every instant. As we increase the frequency (and therefore the Péclet number), the interface temperature variations are more important for bubbles with a low vapour content, although in all cases the non-dimensional values are close to zero. Thus, we can safely assume that the interface temperature is constant for gas bubbles in water irrespective of the forcing frequency. For bubbles with a large vapour content, the situation is different, because the interface temperature is influenced by the mass transfer flux. As this flux decreases when increasing the forcing frequency, there exists a range of intermediate frequencies for which the interface temperature variations become important in order to correctly predict the bubble radial oscillations.

In order to gain further insight into the applicability of the assumption of constant interface temperature, figure 5 compares the solution obtained with the full model with the solution obtained by imposing that the interface temperature remains constant ($\Delta T^I_c = 0$), still considering the mass transfer flux across the interface. The results are shown for a gas/vapour bubble at 25 °C (approximately 0.03 % of vapour content) and 99.9 °C ($Y_0 = 0.99$). While at low ambient temperatures (low vapour content) the results obtained with $\Delta T^I_c = 0$ accurately represent the solution obtained with the full model, we observe significant differences when approaching saturation conditions. In this case the vaporization flux is significant and it is important to include interface temperature variations for an accurate estimation of the phase speed and attenuation at frequencies below the resonance frequency. Only if we decrease frequencies further can the bubble response be assumed to be isothermal and the phase velocities obtained assuming constant temperature accurately represent the solution of the full model. Note that this is not the case for the attenuation, where the interface temperature variations seem to have a significant influence on the predictions and must then always be considered in the predictions.

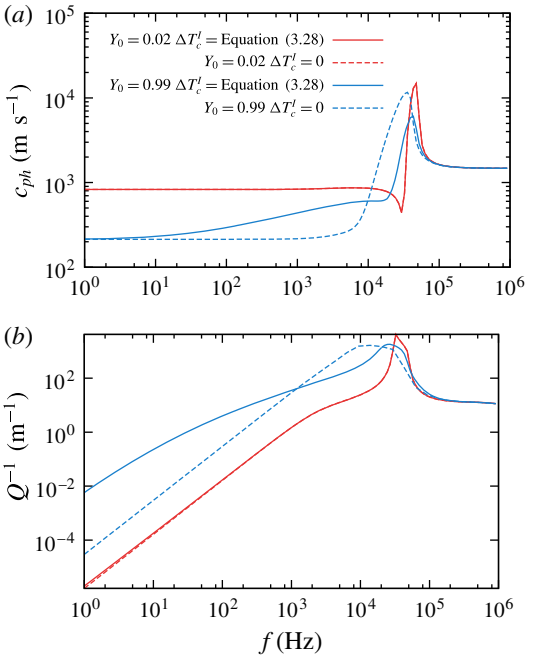

FIGURE 5. (Colour online) Phase speed (*a*) and attenuation curves (*b*) for an air–water system with 100 μm bubbles with concentration $\beta_0 = 10^{-4}$ at 25 °C (red lines, $Y_0 = 0.03$) and 99.9 °C (blue lines, $Y_0 = 0.99$). The continuous lines represent the solution of the full model. The dashed lines represent the solution assuming a constant interface temperature. The two solutions overlap for systems containing gas bubbles, whereas we observe significant differences between them for low-frequency waves propagating in systems with bubbles with a large vapour content.

6. Low-frequency limits

We have seen in the previous section that mass transfer effects are especially important for low-frequency excitations. In this case both the bubble response and the process of wave propagation are significantly influenced by the mass and energy exchange across the interface. In order to gain further insight into the influence of mass transfer at low frequencies, we derive limiting expressions for particular regimes. For frequencies well below the natural frequency and assuming monodisperse mixtures, it is readily shown that (Commander & Prosperetti 1989)

$$\frac{1}{c_m^2} = \frac{1}{c^2} + 4\pi \frac{nR_0}{\omega_0^2}\left(\frac{1 - 2\mathrm{i}\delta\omega}{\omega_0^2}\right). \tag{6.1}$$

The limiting expressions for ω_0 and δ depend on the evaporation flux and the transfer function. The non-dimensional flux across the interface, given by (3.31), is $J_0^* = -J_c^* \Phi$. In the general case, J_c^* has to be obtained from (3.22), which in the low-frequency limit tends to

$$J_c^* \approx \frac{J_{max}^*}{1 - 3J_{max}^* \mathrm{i}\dfrac{1 - Y_0}{Y_0}} \quad \text{when } Sh_D < 1. \tag{6.2}$$

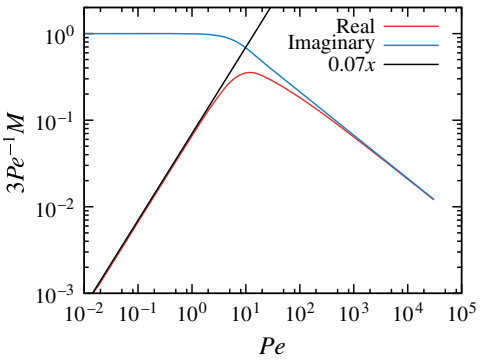

FIGURE 6. (Colour online) Real and imaginary parts of $3Pe^{-1}M$, where $M(Pe) = \sqrt{Pe\,\mathrm{i}}\coth(\sqrt{Pe\,\mathrm{i}}) - 1$, as a function of Pe.

This expression can be further simplified when $J^*_{max} > Y_0/(1-Y_0)/3$, which can be written as a condition for the bubble's Péclet number,

$$Pe_b < Pe_c^I = \frac{3\alpha_{evap}}{\sqrt{2\pi}}(1-Y_0)\frac{R_0\sqrt{r_w T}}{D_b^T}. \tag{6.3}$$

The right-hand side (Pe_c^I) is identified with a critical Péclet number below which transient mass transfer effects are negligible. In this case (6.2) reduces to

$$J_c^* \approx \frac{1}{3}\mathrm{i}\frac{Y_0}{1-Y_0} \quad \text{when } Sh_D < 1 \text{ and } Pe_b < Pe_c^I, \tag{6.4}$$

which is equivalent to the low-frequency solution obtained when assuming equilibrium conditions at the interface (see appendix A). Thus, we write the mass transfer flux across the interface and the transfer function as

$$J_0^* \approx -\frac{1}{3}\mathrm{i}\frac{Y_0}{1-Y_0}\Phi, \tag{6.5}$$

$$\Phi \approx \frac{3(1-Y_0)}{1-(1-Y_0)\Delta T_c^I\dfrac{\gamma-1}{\gamma} - Y_0\Delta H^*_{vap}\Delta T_c^I}, \tag{6.6}$$

which are valid when $Sh_D < 1$ and $Pe_b < \min(1, Pe_c^I)$. Note that, to derive the expression for the transfer function, we have approximated the function $M(Pe) = \sqrt{Pe\,\mathrm{i}}\coth(\sqrt{Pe\,\mathrm{i}}) - 1$ by $M(Pe) \approx (Pe/3)\mathrm{i}$, which is a reasonable assumption for $Pe_b < 1$ (figure 6).

The mass transfer flux and the transfer function are both functions of the interface temperature variations given by (3.28). For low frequencies, $Pe_b < 1$, (3.28) simplifies to

$$\Delta T_c^I \approx \frac{\dfrac{\kappa_b}{\kappa_l}\dfrac{1}{3}\mathrm{i}\left[1+\dfrac{Y_0}{1-Y_0}\Delta H^*_{vap}\dfrac{\gamma}{\gamma-1}\right]Pe_b}{1+\sqrt{Pe_l\mathrm{i}}+\dfrac{\kappa_b}{\kappa_l}\dfrac{1}{3}\mathrm{i}\left[1+\dfrac{Y_0}{1-Y_0}(\Delta H^*_{vap})^2\dfrac{\gamma}{\gamma-1}\right]Pe_b} \quad \text{when } Sh_D < 1 \text{ and } Pe_b < \min(1, Pe_c^I). \tag{6.7}$$

When the interface temperature is isothermal, $\Delta T_c^I = 0$, which is true for $Pe_b \to 0$, the non-dimensional mass flux across the interface and the transfer function for bubbles containing gas and vapour are

$$J_0^* = Y_0 \mathrm{i}, \tag{6.8}$$

$$\Phi \approx 3(1 - Y_0). \tag{6.9}$$

Using these limiting expressions, the final expressions for the phase speed and attenuation in the low-frequency limit are given by

$$c_{ph}^2 = \frac{c^2}{1 + \dfrac{c^2 \beta_0 \rho_l}{(1 - Y_0) p_0}}, \tag{6.10}$$

$$Q^{-1} = 20 \log_{10}(e) \frac{c \beta_0 \delta \omega^2 \rho_l^2 R_0^2}{3 p_0^2 (1 - Y_0)^2 \sqrt{1 + \dfrac{c^2 \beta_0 \rho_l}{(1 - Y_0) p_0}}}. \tag{6.11}$$

For low void fractions ($\beta_0 < p_0(1 - Y_0)/\rho_l c^2$), the phase speed tends to recover the liquid's sound speed. On the contrary, for large void fractions, the phase speed is shown to be proportional to the gas content inside the bubble.

These limiting expressions are expected to represent reasonably well only the solution for dilute systems when $Sh_D < 1$ and $Pe_b < \min(1, Pe_c^I)$ and also when the interface temperature remains constant. This last condition introduces an additional constraint for Pe_b in order to reach the low-frequency limits obtained above. From (6.7), we conclude that we can only assume constant interface temperature when

$$Pe_b \ll Pe_{b,c}^{II} = 3 \frac{1 - Y_0}{Y_0} \frac{\kappa_l}{\kappa_b} \frac{\gamma - 1}{\gamma} \frac{1}{(\Delta H_{vap}^*)^2}. \tag{6.12}$$

Thus, the frequency required to reach the low-frequency limit is expected to be lower in systems with a low liquid thermal conductivity, a large content of vapour in the bubbles and a large enthalpy of vaporization. This effect can be clearly seen in figure 7, where we compare the solution of systems with different non-dimensional values of the enthalpy of vaporization with the solution of a model where the interface temperature is assumed to be isothermal. As expected, all systems tend to the same low-frequency limit for the phase speed, although we need to lower the forcing frequency as the enthalpy of vaporization increases. In particular, in the case of the highest enthalpy of vaporization tested here (twice the enthalpy of vaporization of water), the curves tend to follow the low-frequency limit for gas bubbles at frequencies between 10^3 and 10^4 Hz. At these frequencies, the vaporization flux is limited by heat diffusion from the bulk towards the interface and the bubble dynamic response is controlled mainly by the expansion or compression rather than by mass transfer effects. For lower frequencies, heat has enough time to diffuse and vaporization controls the effective compressibility of the medium. This remark is important if one wants to guarantee the validity of the low-frequency limiting solutions in systems near saturation conditions, where it is not sufficient to satisfy the condition that the excitation frequency is below the bubble's resonance frequency.

It is also interesting to compare the low-frequency limit solutions obtained here with the classical solution for gas bubbles proposed by Wood (1930). Figure 8 compares

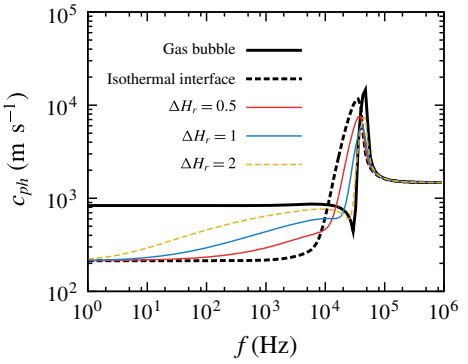

FIGURE 7. (Colour online) Phase speed predictions for systems with 100 μm bubbles with concentration $\beta_0 = 10^{-4}$ at 1 atm. The ambient temperature is fitted to obtain a vapour molar fraction of 0.95. The dashed black line represents the predictions of the model accounting for mass transfer effects that impose constant temperature at the interface. The solutions obtained from the full model are shown for different values of the enthalpy of vaporization, which are given with respect to the enthalpy of vaporization of water, ΔH^0_{vap}, such that $\Delta H_r = \Delta H_{vap}/\Delta H^0_{vap}$. For reference, the continuous black line represents the predictions of the model for a pure gas bubble, which neglects mass transfer effects across the interface.

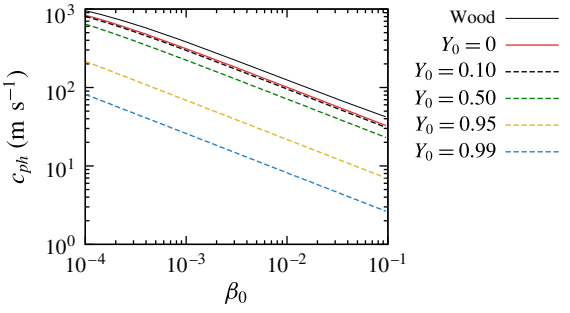

FIGURE 8. (Colour online) Phase speed in the low-frequency limit ($f = 1$ Hz) as a function of the void fraction and various vapour contents for a monodisperse bubble cloud of 100 μm bubbles. For reference the solution of pure gas bubbles and the solution of Wood (1930) is included.

the results obtained with the full model at 1 Hz as a function of the void fraction and the vapour content with the results obtained from Wood's theory. As can be seen, the phase speed is significantly lower for bubbles with a large vapour content than for pure gas bubbles. The effect of the vapour content can also be seen in figure 9, where we see how both phase speed and attenuation converge to the solution for pure gas bubbles with vapour content tending to zero. For the phase velocity, Wood's formula provides a good approximation of the exact solution only when the void fraction is sufficiently low. In the case of attenuation (figure 9), δ depends strongly on the vapour content, increasing by several orders of magnitude compared to the case of pure gas bubbles.

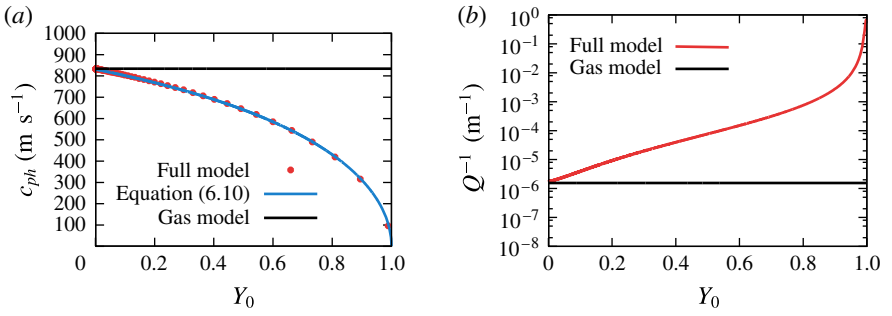

FIGURE 9. (Colour online) Phase speed (*a*) and attenuation (*b*) in the low-frequency limit ($f = 1$ Hz) as a function of the vapour content for a monodisperse bubble cloud of 100 μm bubbles with concentration equal to $\beta_0 = 10^{-4}$. For reference we include the solution of pure gas bubbles and the approximate solution provided by (6.10) and (6.11).

It is also worth mentioning that the limiting solutions of (6.10) and (6.11) differ from the solutions for pure liquid–vapour bubbly liquids obtained by Landau & Lifshitz (1987), who derive an asymptotic solution considering that pressure and temperature at the large scale are coupled through the Clausius–Clapeyron equation. In this study we restrict ourselves to situations where the temperature far from the bubble remains constant, which is a reasonable assumption for dilute systems containing a small amount of gas but it is not applicable for pure vapour bubbles and low frequencies where heating or cooling of the bulk liquid may be relevant. Although the current model for pure vapour bubbles may be extended to account for large-scale thermal effects, for the sake of simplicity we postpone the study of this situation to future investigation. In any case, it is important to note that the limiting solutions reported by Landau & Lifshitz (1987) may be very difficult to obtain experimentally in linear regimes (Coste *et al.* 1990). On the one hand, very small amounts of gas make vapour diffusion inside the bubble the controlling mechanism determining the vaporization flux. As we have seen above, the frequency threshold below which equilibrium conditions prevail inside the bubble at every instant tend to zero for vapour bubbles, which would make it difficult to reach the low-frequency limit in these situations. On the other hand, for the particular case of pure vapour bubbles, the amplitude required to keep the linear regime valid tends to zero for low frequencies. This effect can be clearly seen in figure 10, where we represent the effect of the vapour content on the sensitivity factor S defined from (6.13) as

$$S = \frac{\Delta R}{\Delta p_\infty} = -\frac{1}{\omega_0^2 - \omega^2 + 2\mathrm{i}\delta\omega}\frac{p_{l,0}}{\rho_l R_0^2}. \tag{6.13}$$

This factor represents the non-dimensional amplification factor of the bubble radius oscillation with respect to the external pressure excitation. Given that a pure vapour bubble is unable to reach equilibrium conditions when we perturb the pressure, the bubble tends to grow (or shrink) infinitely as we decrease the frequency. Small amounts of gas serve to kill this singular behaviour, although the sensitivity of the bubble radius oscillation against the pressure pulse is still significantly influenced by the amount of vapour.

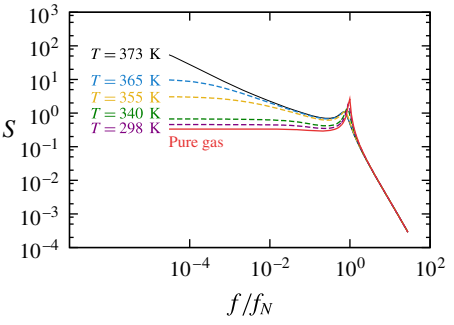

FIGURE 10. (Colour online) Sensitivity factor (as defined in (6.13)) as a function of the vapour content and frequency for a 100 μm gas/vapour bubble. The vapour content is changed by modifying the ambient temperature. As the amount of vapour increases, the bubble radial oscillation is more important for a constant non-dimensional pressure wave amplitude.

7. Conclusions

This paper presents a generalization of the classical linear theory for dilute bubbly liquids that solves for the transient mass transfer effects across the interface as well as the heat transport in the liquid boundary layer. The proposed linear model converges to the solution of the classical linear theory for pure gas bubbles when the vapour content inside the vapour is negligible. Mass transfer effects are shown to play an important role in the phase speed and attenuation curves at frequencies below the bubble resonant frequency. At low frequencies, the phase speed is significantly reduced, while attenuation can increase by various orders of magnitude with respect to the solution obtained when neglecting mass transfer effects.

Simplified solutions are derived for low-frequency excitations. The conditions to be satisfied for these solutions to be valid are also obtained. We show that, to reach the low-frequency limit for the phase speed, it is not sufficient to guarantee that the forcing frequency is lower than the bubble natural frequency. For a general case, the Sherwood number, $Sh_D = \omega R_0^2/D_{w/b}$, must also be smaller than unity and the Péclet number, $Pe_b = \omega R_0^2/D_b^T$, must be smaller than the minimum of two characteristic Péclet numbers, Pe_c^I and Pe_c^{II}, in order to guarantee that thermodynamic equilibrium prevails at every instant. In systems with low liquid conductivity, large enthalpy of vaporization and large vapour content, the frequencies required to reach the isothermal limit can be extremely low. In this low-frequency regime, the bubble response is isothermal and it is possible to derive expressions that capture relatively well the influence of the vapour content on the acoustic properties of the effective medium. Thus, in systems close to saturation conditions and for frequencies below resonance, it is important to solve for the mass transfer flux across the bubble interface and the heat transport equation in the liquid, and to account for the interface temperature variations, in order to accurately obtain the phase speed and attenuation.

Acknowledgements

The authors would like to acknowledge C. Boehm and P. Berthet for their support and discussions.

Appendix A. Mass transfer flux assuming equilibrium conditions at the interface

It is commonly assumed that equilibrium conditions prevail at the interface at every instant. Under these conditions, the partial water vapour pressure at the interface is given at every instant by the saturation pressure at the interface's temperature, $p_{eq}(T^I) = p_b Y_0 (M_b/M_w)$, whose linearized version is

$$\Delta p^I_{eq} = \Delta p_b + \Delta Y^I. \tag{A 1}$$

Replacing Δp^I_{eq} by the expression given by the linear Clausius–Clapeyron relation (2.17),

$$\Delta p_{eq} = \frac{\Delta H_{vap}}{r_w T} \Delta T^I, \tag{A 2}$$

and using (3.16) to express the vapour fraction variations as a function of the mass flux across the interface, we can rewrite (A 1) as

$$J^*_{0,eq} \Delta R = J^*_{c,eq} (\Delta H^*_{vap} \Delta T^I_c - 1) \Delta p_b, \tag{A 3}$$

where

$$J^*_{c,eq} = \left[\frac{Sh_D}{\sqrt{\mathrm{i}Sh_D} \coth(\sqrt{\mathrm{i}Sh_D}) - 1} \frac{1 - Y_0}{Y_0} \right]^{-1}. \tag{A 4}$$

For low frequencies ($Sh_D < 1$), this equation simplifies to

$$J^*_{c,eq} \approx \frac{1}{3} \mathrm{i} \frac{Y_0}{1 - Y_0} \quad \text{when } Sh_D < 1. \tag{A 5}$$

Appendix B. Low-frequency limit of the mass transfer flux assuming thermodynamic equilibrium inside the bubble

The limiting solution of the mass transfer flux for low frequencies can also be obtained by assuming that: (i) the temperature of the bubble remains constant at every instant and equal to the reference temperature, and (ii) the vapour pressure inside the bubble is maintained at every instant. Thus, the water vapour mass can be obtained as

$$m_w = \frac{p_w V}{r_w T}. \tag{B 1}$$

Because only the bubble volume changes, the flux is obtained as

$$J = \frac{\dot{m}_w}{4\pi R_b^2} = \frac{p_w}{r_w T} \dot{R}_b. \tag{B 2}$$

Linearizing the expression above we find

$$J_0 \Delta R = \frac{m_w}{V} \omega \mathrm{i} R_0 \Delta R, \tag{B 3}$$

which in non-dimensional form reads

$$J^*_0 = \frac{J_0}{R_b \rho_{b,0} \omega} = Y_0 \mathrm{i}. \tag{B 4}$$

REFERENCES

AINSLIE, M. A. & LEIGHTON, T. G. 2011 Review of scattering and extinction cross-sections, damping factors, and resonance frequencies of a spherical gas bubble. *J. Acoust. Soc. Am.* **130** (5), 3184–3208.

ANDO, K., COLONIUS, T. & BRENNEN, C. E. 2009 Improvement of acoustic theory of ultrasonic waves in dilute bubbly liquids. *J. Acoust. Soc. Am.* **126**, 69–74.

ARDRON, K. H. & DUFFEY, R. B. 1978 Acoustic wave propagation in a flowing liquid–vapour mixture. *Intl J. Multiphase Flow* **4** (3), 303–322.

CHAPMAN, R. B. & PLESSET, M. S. 1971 Thermal effects in the free oscillations of gas bubbles. *Trans. ASME J. Basic Engng* **93**, 373–376.

CHEYNE, S. A., STEBBINGS, C. T. & ROY, R. A. 1995 Phase velocity measurements in bubbly liquids using a fiber optic laser interferometer. *J. Acoust. Soc. Am.* **97** (3), 1621–1624.

COMMANDER, K. W. & PROSPERETTI, A. 1989 Linear pressure waves in bubbly liquids: comparison between theory and experiments. *J. Acoust. Soc. Am.* **85**, 732–746.

COSTE, C., LAROCHE, C. & FAUVE, S. 1990 Sound propagation in a liquid with vapour bubbles. *Europhys. Lett.* **11** (4), 343–347.

FUSTER, D. & COLONIUS, T. 2011 Modeling bubble clusters in compressible liquids. *J. Fluid Mech.* **688**, 352–589.

FUSTER, D., CONOIR, J. M. & COLONIUS, T. 2014 Effect of direct bubble–bubble interactions on linear-wave propagation in bubbly liquids. *Phys. Rev.* E **90** (6), 063010.

FUSTER, D., HAUKE, G. & DOPAZO, C. 2010 Influence of accommodation coefficient on nonlinear bubble oscillations. *J. Acoust. Soc. Am.* **128**, 5–10.

GUMEROV, N. A., HSIAO, C. T. & GOUMILEVSKI, A. G. 2001 Determination of the accomodation coefficient using vapor/gas bubble dynamics in an acoustic field. Technical Report 1. California Institute of Technology, DYNAFLOW, Inc., Fulton, MD; see also URL http://gltrs.grc.nasa.gov/GLTRS (last viewed 9 May 2015).

HAO, Y. & PROSPERETTI, A. 1999 The dynamics of vapor bubbles in acoustic pressure fields. *Phys. Fluids* **11** (8), 2008–2019.

HAUKE, G., FUSTER, D. & DOPAZO, C. 2007 Dynamics of a single cavitating and reacting bubble. *Phys. Rev.* E **75**, 066310,1-14.

HERTZ, H. 1982 Über die Verdunstug der Flüssigkeiten, Inbesondere des Quecksilbers im lufteren Räume [On the evaporation of fluids, especially of mercury, in vacuum spaces]. *Ann. Phys.* **17**, 177–193.

KIEFFER, S. W. 1977 Sound speed in liquid–gas mixtures: water–air and water–steam. *J. Geophys. Res.* **82** (20), 2895–2904.

KNUDSEN, M. 1915 Maximum rate of vaporization of mercury. *Ann. Phys.* **47**, 697–705.

KUSTER, G. T. & TOKSÖZ, M. N. 1974 Velocity and attenuation of seismic waves in two-phase media: Part I. Theoretical formulations. *Geophysics* **39** (5), 587–606.

LANDAU, L. D. & LIFSHITZ, E. M. 1987 *Fluid Mechanics*. Pergamon.

LEROY, V., STRYBULEVYCH, A., PAGE, J. H. & SCANLON, M. G. 2008 Sound velocity and attenuation in bubbly gels measured by transmission experiments. *J. Acoust. Soc. Am.* **123**, 1931–1940.

LYNNWORTH, L. C. 2013 *Ultrasonic Measurements for Process Control: Theory, Techniques, Applications*. Academic.

MECREDY, R. C & HAMILTON, L. J. 1972 The effects of nonequilibrium heat, mass and momentum transfer on two-phase sound speed. *Intl J. Heat Mass Transfer* **15** (1), 61–72.

PRESTON, A. T., COLONIUS, T. & BRENNEN, C. E. 2007 A reduced order model of diffusive effects on the dynamics of bubbles. *Phys. Fluids* **19**, 123302,1-19.

PROSPERETTI, A. 1977 Thermal effects and damping mechanisms in the forced radial oscillations of gas bubbles in liquids. *J. Acoust. Soc. Am.* **61**, 17–27.

PROSPERETTI, A. 1982 A generalization of the Rayleigh–Plesset equation of bubble dynamics. *Phys. Fluids* **25** (3), 409–410.

PROSPERETTI, A. 2015 The speed of sound in a gas–vapor bubbly liquid. *Interface Focus* 20140024, doi:10.1098/rsfs.2015.0024.

PROSPERETTI, A., CRUM, L. A. & COMMANDER, K. W. 1988 Nonlinear bubble dynamics. *J. Acoust. Soc. Am.* **83**, 502–514.

PROSPERETTI, A. & HAO, Y. 2002 Vapor bubbles in flow and acoustic fields. *Ann. N.Y. Acad Sci.* **974** (1), 328–347.

SANGANI, A. S. 1991 A pairwise interaction theory for determining the linear acoustic properties of dilute bubbly liquids. *J. Fluid Mech.* **232**, 221–284.

SAUREL, R., PETITPAS, F. & ABGRALL, R. 2008 Modelling phase transition in metastable liquids: application to cavitating and flashing flows. *J. Fluid Mech.* **607**, 313–350.

SILBERMAN, E. 1957 Sound velocity and attenuation in bubbly mixtures measured in standing wave tubes. *J. Acoust. Soc. Am.* **29** (8), 925–933.

VAN WIJNGAARDEN, L. 1968 On the equations of motion for mixtures of liquid and gas bubbles. *J. Fluid Mech.* **33** (3), 465–474.

WILSON, P. S., ROY, R. A. & CAREY, W. M. 2005 Phase speed and attenuation in bubbly liquids inferred from impedance measurements near the individual bubble resonance frequency. *J. Acoust. Soc. Am.* **117** (4), 1895–1910.

WOOD, A. B. 1930 *A Textbook of Sound*. G. Bell and Sons.

YASUI, K. 1997 Alternative model of single sonoluminiscence. *Phys. Rev.* E **56** (6), 6750–6760.

ZHANG, D. Z. & PROSPERETTI, A. 1997 Momentum and energy equations for disperse two-phase flows and their closure for dilute suspensions. *Intl J. Multiphase Flow* **23**, 425–453.